Elucidation of the Molecular and Toxico-pathological Role of Indoxyl Sulfate in Unilateral Ureter Obstruction-induced Renal Fibrosis

HUIXIAN HOU

Department of Clinical Pharmaceutical Sciences

Graduate School of Pharmaceutical Sciences

Kumamoto University

2023

Elucidation of the Molecular and Toxico-pathological Role of Indoxyl Sulfate in Unilateral Ureter Obstruction-induced Renal Fibrosis

Department of Clinical Pharmaceutical Sciences, Graduate School of Pharmaceutical Sciences, Kumamoto University

HUIXIAN HOU

Background: Chronic kidney disease (CKD) is a progressive condition that affects over 800 million people worldwide and represents an especially large burden in low- and middle-income countries. Increased efforts for better prevention and treatment should be made because of the large number of affected people and the serious negative effects of CKD. Renal fibrosis is considered the final manifestation in patients with CKD, and its prevention is vital for controlling CKD progression. Currently, many therapeutic interventions have been done in animal models and appeared to be effective, however, it is difficult to translate these therapies into CKD patients. Thus, new insights into the molecular mechanisms of renal fibrosis and therapeutic strategies are urgently needed. Our laboratory has reported that indoxyl sulfate (IS) accumulates significantly in serum and kidney of acute kidney injury (AKI) and CKD animal models. However, the effect of IS on progressive renal fibrosis remains unknown. IS is a typical sulfate-conjugated uremic solute and is produced in the liver via CYP2A6/2E1-dependent oxidative metabolism of gut-derived indole, followed by sulfotransferase (SULT) 1A1-mediated sulfate transfer to indoxyl. Therefore, I investigated the toxico-pathological role of IS in renal fibrosis using *Sult1a1*-KO mice and the underlying mechanisms.

Methods: I established 2-week unilateral ureter obstruction (UUO) model on WT and *Sult1a1*-knock out (KO) mice. To confirm whether IS could accumulate in this model, serum and kidney IS concentrations were assessed by LC-MS/MS. Renal fibrosis was assessed by Sirius red staining and the expression of related markers. Inflammation was assessed by the expression of cytokines. Oxidative stress was assessed by the expression of oxidative stress markers and DHE, 4-HNE, 8-OHdG staining. In addition, macrophage polarization and Wnt/β-catenin signaling activation, which may be in-

process interactions in IS-induced renal fibrosis, were examined. Furthermore, to confirm the impact of erythropoietin (EPO) on renal fibrosis, the time-dependent expression of EPO was evaluated, and recombinant human erythropoietin (rhEPO) was administered to the UUO model.

Results: BUN had no increase after UUO surgery in WT and *Sult1a1*-KO mice. While UUO surgery induced significant upregulation in hepatic *Sult1a1*. IS was successfully accumulated in the serum and obstructed kidney. Inflammation and renal fibrosis were exacerbated in WT mice, with an accumulation of IS in the kidney; however, they were significantly suppressed in *Sult1a1*-KO mice. Oxidative stress increased in the WT UUO model but did not significantly differ from it in the *Sult1a1*-KO mice. In addition, although F4/80 was observed no changes, $CD80^+$ expression was downregulated and $CD206^+$ expression was upregulated in *Sult1a1*-KO mice. Sfrp5, an antagonist of Wnt protein, its expression was upregulated, β-catenin expression was downregulated in *Sult1a1*-KO mice. Moreover, EPO mRNA expression was improved considerably in *Sult1a1-KO* mice. The administration of rhEPO further attenuated UUO-induced renal fibrosis in *Sult1a1*-KO mice.

Conclusions: This study demonstrated that UUO-induced renal fibrosis was alleviated in *Sult1a1*-KO mice with a decreased accumulation of IS. Inactivated Wnt/β-catenin signal, infiltrated $CD206^+$ macrophages and improved EPO produce capacity were corelated with the attenuated renal fibrosis in *Sult1a1*-KO mice. Our findings confirmed the pathological role of IS in renal fibrosis and identified SULT1A1 as a new therapeutic target enzyme for the prevention and attenuation of renal fibrosis.

ABBREVIATIONS

AKI	Acute kidney injury
AhR	Aryl hydrocarbon receptor
α-SMA	α-smooth muscle actin
BUN	Blood urea nitrogen
CKD	Chronic kidney disease
Col1a1	Collagen 1a1
DHE	Dihydroethidium
EPO	Erythropoietin
ESRD	End-stage renal disease
GABP	GA-binding protein
HO-1	Heme oxygenase
HUVECs	Human umbilical vein endothelial cells
IL-1β	Interleukin-1β
IL-6	Interleukin-6
IR	Ischemia-reperfusion
IS	Indoxyl sulfate
LC-MS/MS	Liquid chromatography tandem mass spectrometry
MS	Mass spectrometry
Nox	NADPH oxidase
OAT	Organic anion transporter
PBS	Phosphate-buffered saline
PCS	*p*-Cresol sulfate
rhEPO	Recombinant erythropoietin
ROS	Reactive oxygen species
SDS	Sodium dodecyl sulfate
Sfrp5	Secreted frizzled-related protein 5
Sp1	Specificity protein 1

Sult1a1	Sulfotransferase 1a1
TBS	Tris-buffered saline
TBS-T	Mixture of tris-buffered saline and tween
TNF-α	Tumor necrosis factor-α
UUO	Unilateral ureteral obstruction
UPLC-MS/MS	Ultra-performance liquid chromatography tandem mass spectrometry
XO	Xanthine oxidase
WT	Wilde type
4-HNE	4-Hydroxynonenal
8-OHdG	8-Hydroxy-2’-deoxyguanosine

Contents

Chapter 1 Introduction

Numerous epidemiological studies indicate that chronic kidney disease (CKD) prevalence is increasing globally.[1, 2] Up to 2022, CKD was affecting >10% of the general population worldwide, amounting to >800 million individuals.[3] The main treatments for CKD patients are primary disease-associated medicine, lifestyle changes, and diet therapy; only conservative treatment is used. Thus, many patients eventually progress to end-stage kidney disease (ESRD), a devastating condition that requires lifelong dialysis or kidney transplantation. Renal fibrosis is recognized as a final manifestation among CKD patients, regardless of the initial causes of CKD.[4] Moreover, the prevalence of renal fibrosis is 1 in 6 persons globally.[5] Although many studies have provided effective therapies for renal fibrosis established on animal models, an approved treatment for CKD patients is very few.[6] Understanding the mechanisms behind renal fibrosis is essential for developing therapies to prevent or reverse this process and slow the progression of CKD to ESRD.

Indoxyl sulfate (IS), a typical sulfate-conjugated uremic toxin,[7, 8] is thought to be a risk factor for renal disease progression because it accumulates in the body during renal dysfunction and causes oxidative stress.[9] IS in the blood circulation was absorbed into proximal tubular cells *via* the organic anion transporter (OAT)1 and OAT3 and then excreted into the urine.[10] When kidney function is compromised, IS accumulates significantly in the blood and kidney of the AKI model, leading to kidney

damage.[11] Several clinical studies revealed that patients with CKD having a high indoxyl sulfate (≥ 6.124 mg/L) were significantly associated with renal progression to dialysis.[12, 13] However, the effect of IS on renal fibrosis has not been widely investigated in vivo. In addition, IS removal by dialysis is difficult due to its high protein binding rate, particularly to serum albumin (~95%).[14] On the other hand, AST-120, a charcoal adsorbent, which adsorbs IS precursors in the gut, reduces serum IS levels in patients with CKD and the risk of CKD progress to the end stage renal disease.[15, 16] However, AST-120 requires large doses, an adult must take 6 g per day, making it challenging to maintain adherence; furthermore, it nonspecifically adsorbs concomitant medications,[17] among other clinical problems. Consequently, it is acknowledged that developing new methods or strategies to lower or remove the systemic accumulation of IS in patients with kidney disease and uremia is an urgent issue.

Here, I focus on the production of IS. IS is produced in the liver by CYP2A6/2E1-dependent oxidative metabolism of gut-derived indole, followed by sulfotransferase (SULT) 1A1-mediated sulfate transfer to indoxyl (Figure 1).

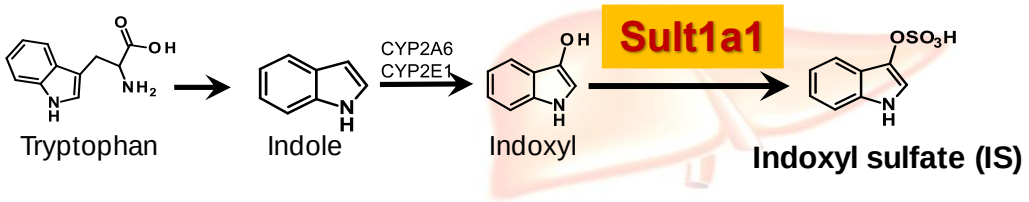

Figure 1. Production pathway of IS

Our previous study reported that the concentration of IS in the serum and kidney was lower in *Sult1a1*-deficient (*Sult1a1*-KO) cisplatin mice,[18] and the increase of IS level could be due to the downregulation of renal organic ion transporters and central nervous system toxicities in cisplatin-induced AKI model rats.[19, 20] Moreover, the inhibition of IS production elicited a renoprotective effect in the ischemic AKI model.[11] Notably, the in-depth mechanism of IS on progressive renal fibrosis has not been well demonstrated.

In this study, I investigated the toxico−pathological role of IS in renal fibrosis using *Sult1a1*-KO mice and the underlying mechanisms.

Chapter 2 Results

Section 1 Effect of *Sult1a1*-KO on the pathology of UUO mice

This study aims to investigate the toxico-pathological role of IS in renal fibrosis. Therefore, a unilateral ureteral obstruction (UUO) model that induces progressive renal fibrosis was used in this study. A lot of studies were using UUO model to investigate the molecular mechanisms underlying renal fibrosis and screen the anti-renal fibrosis drugs.[21-23] Complete UUO triggers a rapid chain of events in the obstructed kidney, resulting in reduced renal blood flow and glomerular filtration rate within 24 hours.[24] This is followed by hydronephrosis, interstitial inflammatory infiltration, and tubular cell death within a few days.[25]

In UUO mice, the kidney function of the obstructed UUO kidney is abolished. In contrast, the contralateral kidney still maintains normal kidney function. In this section, due to the contralateral kidney, I firstly confirmed whether IS could accumulate in UUO mice. And then, examined the effect of *Sult1a1*-KO on UUO-induced inflammatory infiltration and renal fibrosis.

Result 1. Effect of *Sult1a1*-KO on IS accumulation in UUO mice

UUO surgery was performed in WT and *Sult1a1*-KO mice. Serum and kidney tissue samples were collected after 14 days. There was no significant increase in serum BUN levels in the WT UUO and *Sult1a1*-KO UUO groups (Figure 2A). *Sult1a1* mRNA expression was increased in the WT UUO group and significantly decreased in the *Sult1a1*-KO UUO group (Figure 2B). The serum and renal IS concentrations were elevated in the WT UUO group; however, the IS concentration in the serum and kidney of the *Sult1a1*-KO UUO group was lower than that in the WT UUO group (Figure 2C, D). In the liver, an increasing trend in IS concentration was observed in the WT UUO group (Figure 2E). In contrast, a decreasing trend was observed in the *Sult1a1*-KO UUO group compared to the WT UUO group. These results indicated that IS concentration in the serum and kidney was decreased in *Sult1a1*-KO mice even after UUO surgery, proving that *Sult1a1* is involved in the production/accumulation of IS under UUO-induced kidney injury.

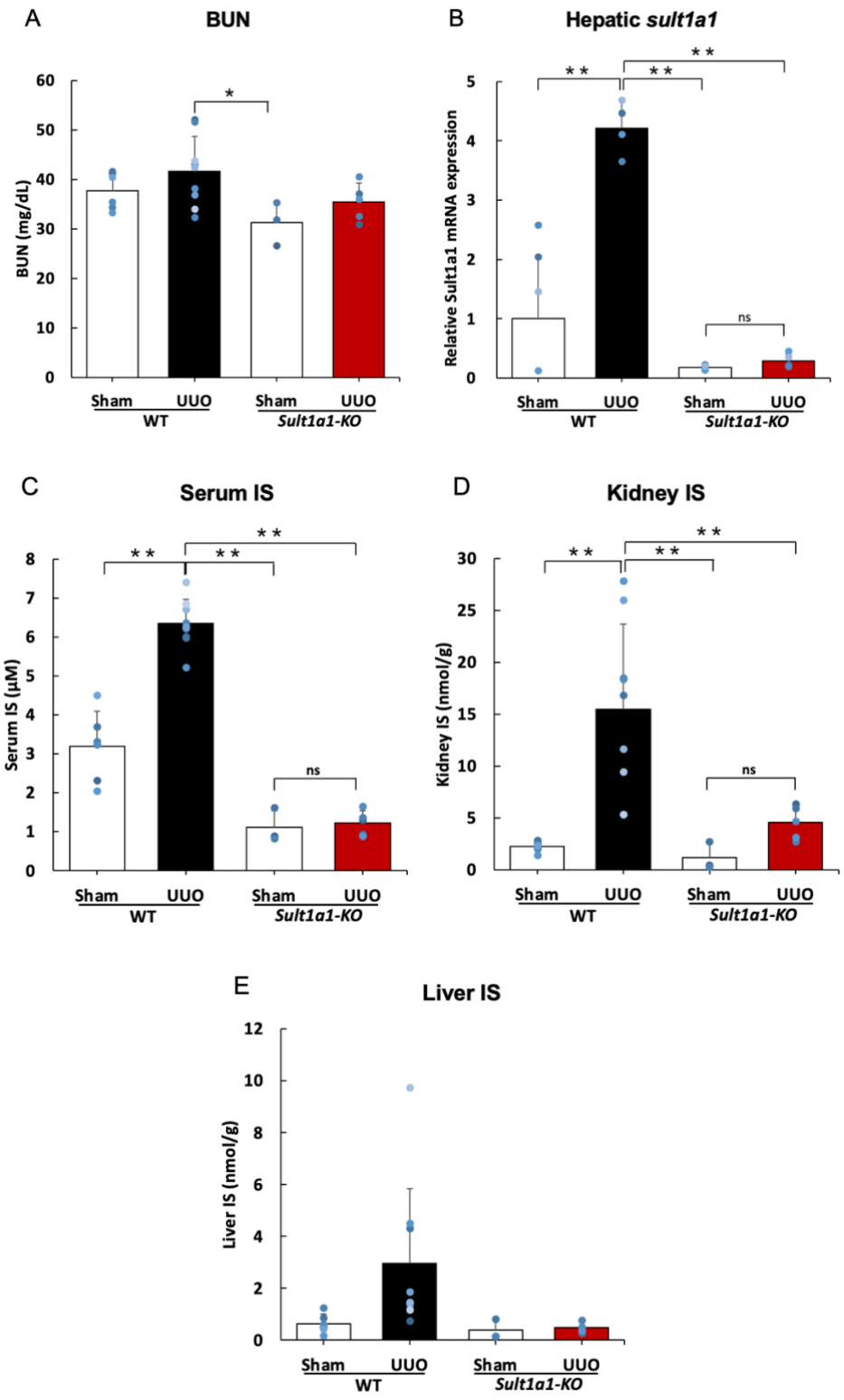

Figure 2. Effect of *Sult1a1*-KO on IS concentration in serum and kidney. (A)S*ult1a1* gene expression checked by RT-PCR. (B) Serum BUN concentration checked in WT and *Sult1a1*-KO mice. (C, D, E) IS concentration in serum, kidney and liver calculated by LC-MS/MS. Each value represents the mean ± S.D. of 3-9 mice. *$p < 0.05$, **$p < 0.01$, ns: not significant

Result 2. Effect of *Sult1a1*-KO on UUO-induced renal fibrosis

The UUO model exhibits prominent renal fibrosis. Thus, I examined whether UUO-induced renal fibrosis could be improved in *Sult1a1*-KO mice. Renal fibrosis markers, col1a1 and fibronectin, were highly expressed in the WT UUO group and were significantly suppressed in the *Sult1a1*-KO UUO group (Figure 3A, B). Sirius red staining (Figure 3C) revealed marked collagen deposition (red part) in the kidneys of the WT UUO group. In contrast, in the kidneys of the *Sult1a1*-KO UUO group, the deposition was suppressed significantly. In addition, the protein expression of α-SMA, a marker of myofibroblasts (Figure 3D), demonstrated decreased fibrosis in the kidneys of *Sult1a1*-KO mice. These data indicated that UUO-induced renal fibrosis was significantly alleviated in *Sult1a1*-KO mice.

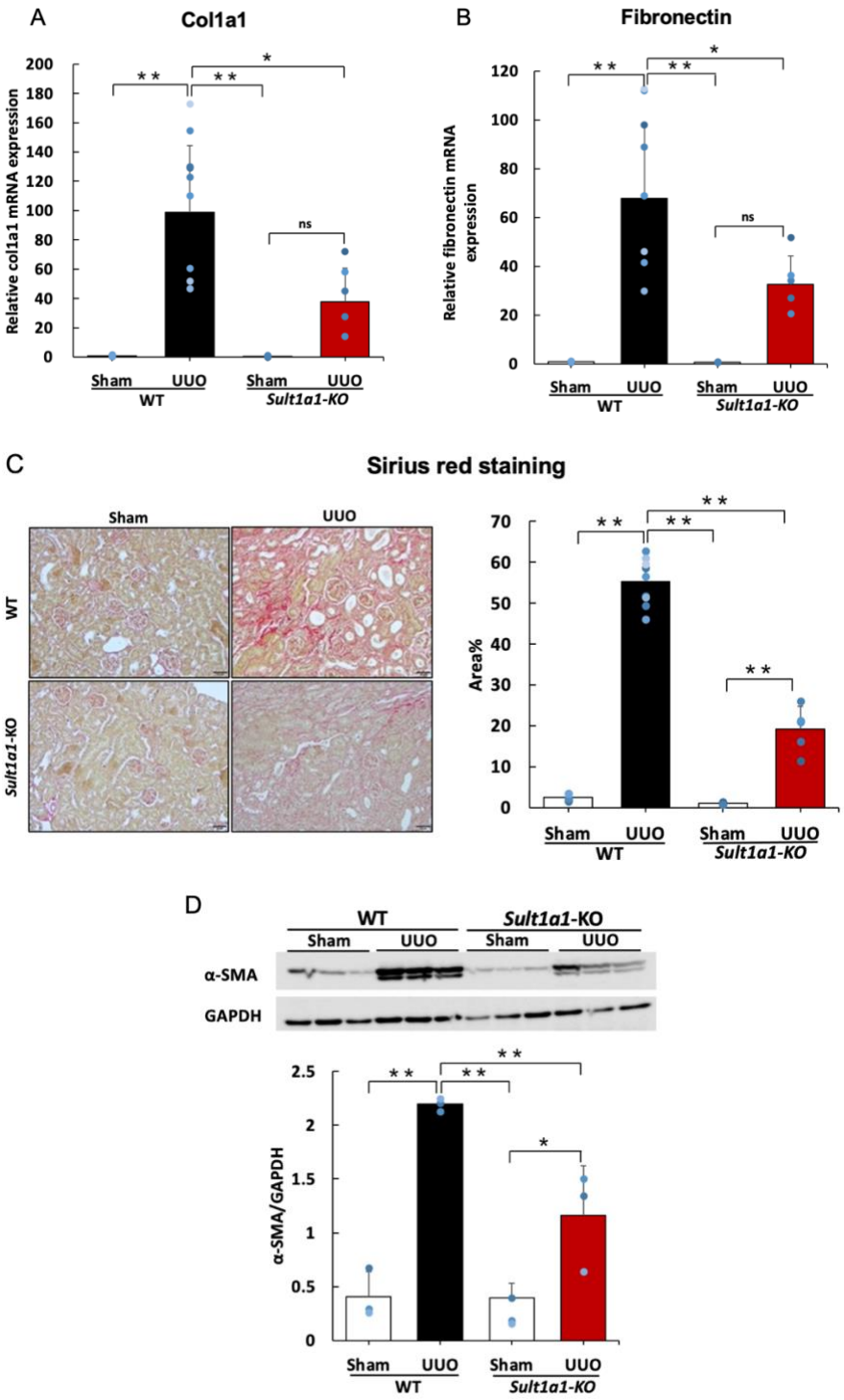

Figure 3. Effect of *Sult1a1*-KO on renal fibrosis induced by UUO. (A, B) Gene expression of renal fibrosis markers (col1a1, fibronectin) assessed by RT-PCR. (C) Collagen deposition (the red area) in the kidney confirmed by Sirius red staining. The scale bar = 50μm. (D) Western blot experiment confirmed the expression of α-SMA. Each value represents the mean ± S.D. of 3–9 mice. $^{*}p < 0.05$, $^{**}p < 0.01$

Result 3. Effect of *Sult1a1*-KO on UUO-induced inflammation

Since *Sult1a1* deficiency has been shown to suppress renal fibrosis, I used RT-PCR to evaluate inflammation, which is known to be associated with renal fibrosis. The gene expression of TNF-α and IL-1β increased significantly in the kidneys of WT UUO mice, which was markedly suppressed in the *Sult1a1*-KO UUO group kidneys (Figure 4A, B). The expression of IL-6 demonstrated a similar tendency (Figure 4C), suggesting that the inflammatory responses were alleviated when IS did not accumulate in the serum and kidney. These data indicated that UUO-induced inflammation and renal fibrosis were partly improved with decreased IS accumulation.

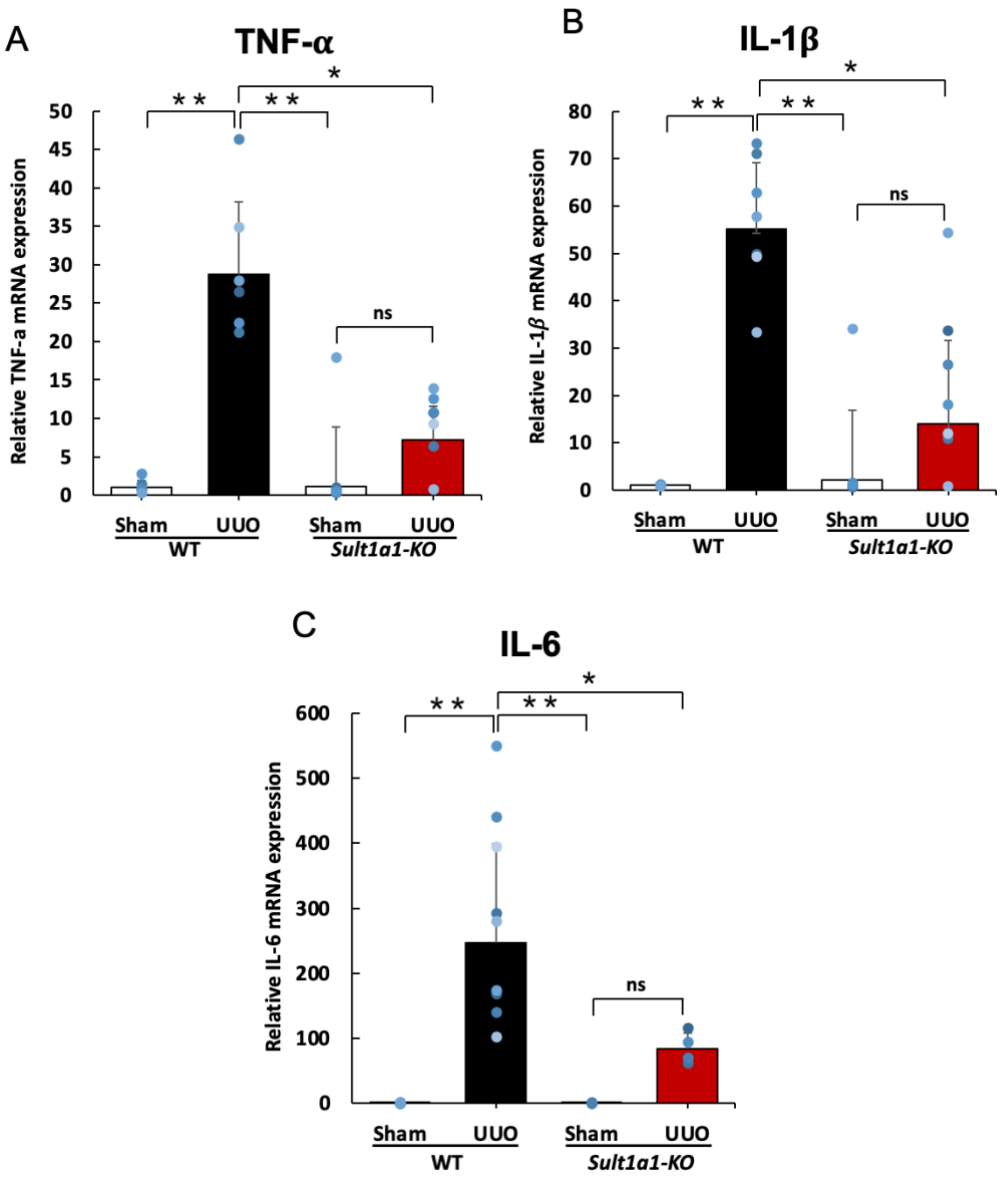

Figure 4. Effect of *Sult1a1*-KO on inflammation. (A, B, C) Gene expression of inflammatory cytokines (TNF-α, IL-1β, IL-6) checked by RT-PCR. Each value represents the mean ± S.D. of 3–9 mice. *$p < 0.05$, **$p < 0.01$, ns: not significant

Result 4. Effect of *Sult1a1*-KO on oxidative stress

Oxidative stress was also evaluated since it has been reported that oxidative stress are involved in renal fibrosis. IS is a ligand of aryl hydrocarbon receptor (AhR) and inducing oxidative stress in cisplatin-induced AKI mice.[18] In WT UUO model, the expression of AhR was increased at the transcriptional level and presented a decreased tendency in *Sult1a1*-KO UUO mice (Figure 5A). Although WT UUO mice displayed increased oxidative stress as confirmed by the expression of HO-1, XO, Nox1 and Nox2, their expression showed no significant differences between WT and *Sult1a1*-KO UUO mice (Figure 5B-5E). Moreover, ROS was increased in UUO model as confirmed by DHE staining and showed no difference between WT and *Sult1a1*-KO mice (Figure 5F). Lipid oxidative stress marker, 4HNE, and DNA damage oxidative stress marker, 8-OHdG, both of their expression showed no differences in WT and *Sult1a1*-KO mice (Figure 5F). All of these results confirming that attenuated renal fibrosis in *Sult1a1*-KO UUO mice has no relationship with increased oxidative stress.

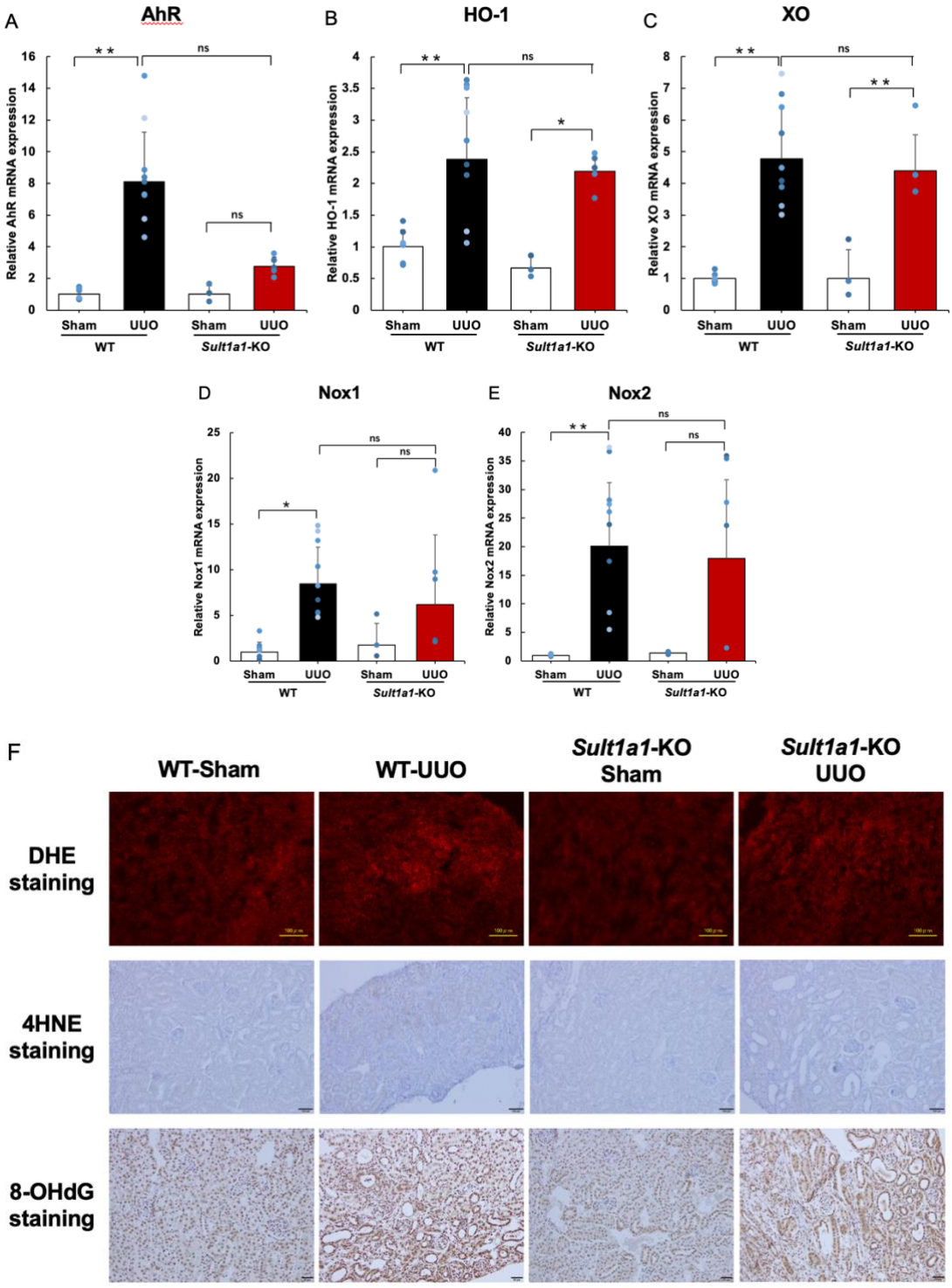

Figure 5. Effect of *Sult1a1*-KO on IS-induced oxidative stress. (A-E) Gene expression of AhR and oxidative stress markers (HO-1, XO, Nox1, 2) checked by RT-PCR. **(F)** DHE staining and immunostaining of 4HNE and 8-OHdG. The scale bar = 100μm. Each value represents the mean ± S.D. of 3–9 mice. *$p < 0.05$, **$p < 0.01$, ns: not significant

Section 2 The mechanisms underlying reduced renal fibrosis in *Sult1a1*-KO mice

Renal inflammation is induced as a protective response to a wide range of injuries in an attempt to eliminate the cause and promote repair, but ongoing inflammation, regardless of the underlying etiology, promotes progressive renal fibrosis.[26] In section 1, I have observed the decreased expression of inflammatory cytokines in *Sult1a1*-KO mice (Figure 4). The degree of macrophage infiltration correlates with both the severity of renal damage and the extent of renal fibrosis.[27, 28] Moreover, the infiltration of macrophages was reported to produce cytokines responsible for tubular apoptosis and fibroblast proliferation and activation.[29] And IS was found to promote proinflammatory macrophage activation.[30] Therefore, I then investigated the infiltration of macrophages and apoptosis in section 2.

On the other hand, Wnt/β-Catenin signaling was reported to promote UUO-induced renal interstitial fibrosis.[31] IS could suppress endothelial Wnt signaling by increasing β-catenin polyubiquitination and proteosomal degradation.[32] In addition, fibronectin, which is the target gene of Wnt signaling, exhibited lower expression in *Sult1a1*-KO mice (Figure 3B). Thus, I was assessed the effect of *Sult1a1*-KO on the activation of Wnt/β-catenin signaling.

Result 5. Effect of *Sult1a1*-KO on macrophage polarization

Inflammatory cytokines were evaluated for macrophage activation, as they exhibited significant differences between WT and *Sult1a1*-KO mice. Although the expression of F4/80 demonstrated no significant differences between the WT UUO group and *Sult1a1*-KO UUO group (Figure 6A), the expression of $CD80^+$, the marker of M1 macrophage, was significantly decreased in *Sult1a1*-KO UUO mice (Figure 6B); $CD206^+$, an anti-inflammatory macrophage-related surface marker, was significantly increased in the *Sult1a1*-KO UUO group compared to the WT UUO group (Figure 6C). In addition, Immunostaining for $CD206^+$ macrophages revealed similar results, with significantly increased invasive areas in the *Sult1a1*-KO UUO group compared to the WT UUO group (Figure 6D). These results revealed that the infiltration of $CD206^+$ macrophages could play a key role in the attenuation of inflammation and renal fibrosis in *Sult1a1*-KO UUO mice. Furthermore, I confirmed apoptosis using TUNEL staining. Apoptosis, which increased in the WT UUO group, was significantly decreased in the *Sult1a1*-KO UUO group (Figure 6E), suggesting that apoptosis was suppressed with reduced IS accumulation.

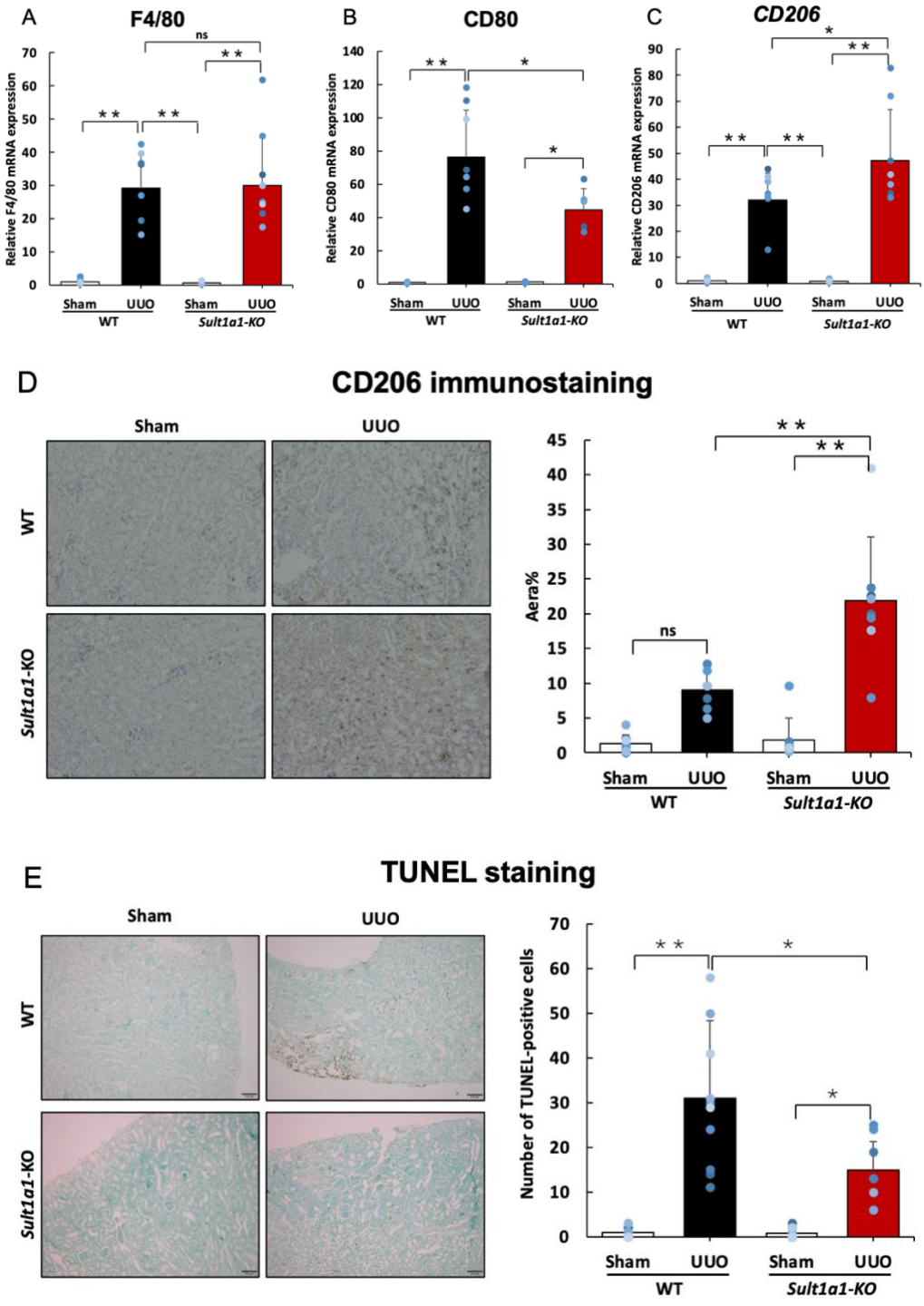

Figure 6. Effect of *Sult1a1*-KO on UUO-induced CD206$^+$ macrophage infiltration. (A, B, C) Gene expression of F4/80, CD80 and CD206 checked by RT-PCR. (D) immunostaining of CD206. The scale bar = 50 μm. (E) apoptotic cells checked by TUNEL staining. The scale bar = 50 μm. Each value represents the mean ± S.D. of 7–8 mice. *$p < 0.05$, **$p < 0.01$, ns: not significant

Result 6. Effect of *Sult1a1*-KO on the activation of Wnt/β-catenin signaling

Notably, the activation of Wnt/β-catenin signaling triggers tubular epithelial cell transition to mesenchymal or senescent phenotype and promotes renal fibrosis.[33] I considered whether the Wnt/β-catenin signal affects the attenuated renal fibrosis in *Sult1a1*-KO mice. Interestingly, although the expression of Wnt4, which encodes a protein of the Wnt family, was comparable in the WT UUO and *Sult1a1*-KO UUO groups (Figure 7A), the expression of sfrp5, which acts as an antagonist of the Wnt protein, was significantly increased in the *Sult1a1*-KO UUO group (Figure 7B). Furthermore, despite the gene expression of β-catenin being similar in the UUO and *Sult1a1*-KO UUO groups (Figure 7C), protein expression was significantly decreased in the *Sult1a1*-KO UUO group (Figure 7D), suggesting that a portion of the Wnt/β-catenin signaling pathway was inactivated when IS accumulation was decreased.

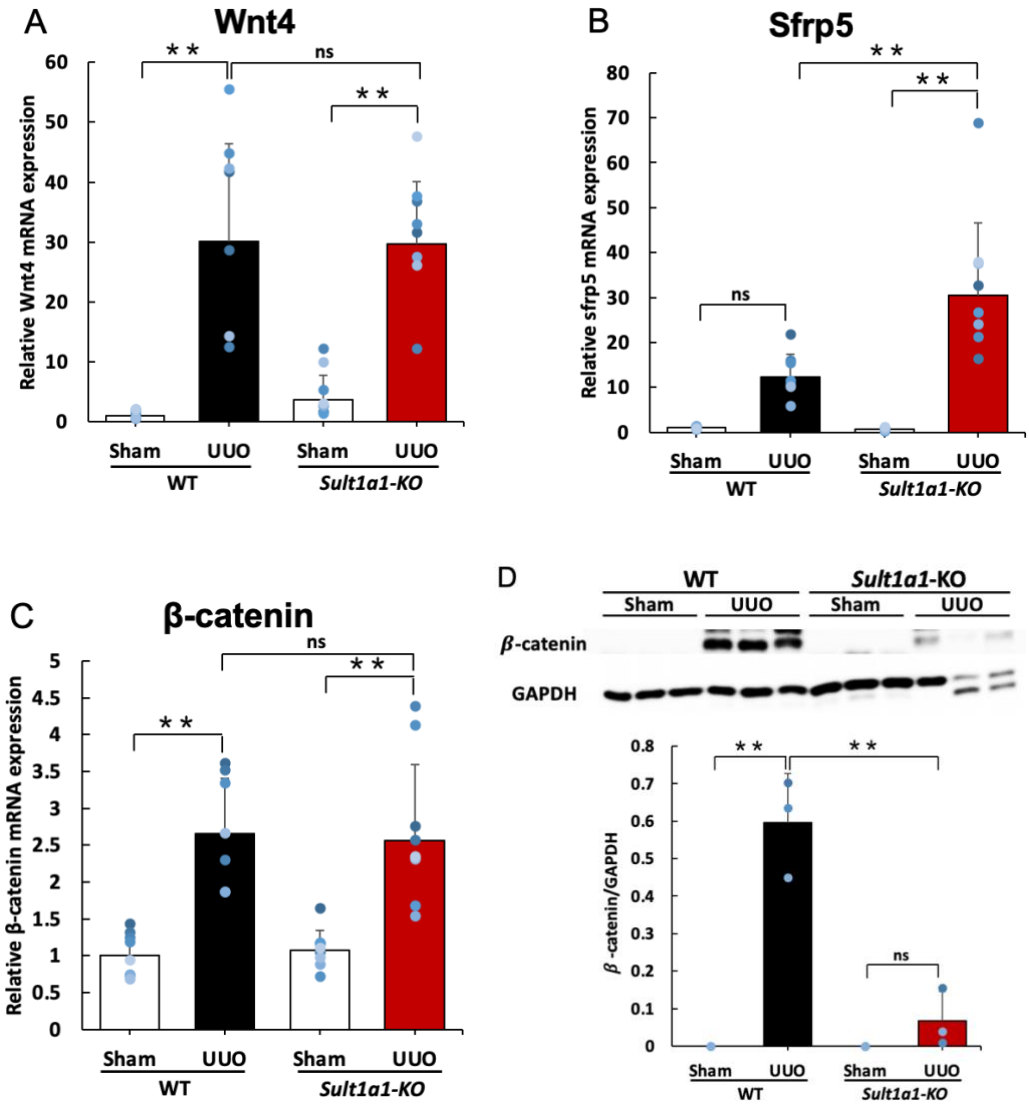

Figure 7. Effect of *Sult1a1*-KO on Wnt/β-catenin signaling activation. (A) Gene expression of Wnt4 checked by RT-PCR. (B) Gene expression of sfrp5 checked by RT-PCR. (C) Gene expression of β-catenin checked by RT-PCR. (D) Protein expression of β-catenin checked by Western blot. Each value represents the mean ± S.D. of 7–8 mice. *$p < 0.05$, **$p < 0.01$, ns: not significant

Section 3 The relationship between EPO and renal fibrosis using *Sult1a1*-KO mcie

Fibroblast dysfunction causes renal fibrosis and anemia in CKD. Renal fibrosis is caused by an increase in myofibroblasts, whereas renal anemia is caused by a decrease in the production of fibroblast-derived erythropoietin (EPO), a hormone that stimulates erythropoiesis.[34] In 2-week UUO model, the expression of EPO was decreased while the expression of α-SMA was increased, indicating the possibility that decreased EPO expression had effect on renal fibrosis formation.[35] Moreover, IS significantly suppressed EPO mRNA expression at non-cytotoxic concentrations in HepG2 cells.[36] However, the relationship among IS, EPO and renal fibrosis has not been widely investigated. Thus, in this part, I firstly assessed the time-dependent expression of EPO in WT and *Sult1a1*-KO UUO mice. And then, administrate recombinant erythropoietin (rhEPO) into WT and *Sult1a1*-KO mice to confirm the relationship among IS, EPO and UUO-induced renal fibrosis.

Result 7. Effect of *Sult1a1*-KO on EPO production and renal fibrosis

It has been reported that the plasticity of renal EPO-producing cells governs fibrosis.[35] Therefore, I evaluated the time-dependent expression of EPO mRNA. Despite a decrease in EPO expression in the WT UUO group after UUO surgery, EPO expression was significantly improved by day 14 in the *Sult1a1*-KO UUO group (Figure 8A). To further investigate the role of EPO in IS-exacerbated renal fibrosis, I administered rhEPO to WT and *Sult1a1*-KO mice, as described in protocol 3. Increased α-SMA in the WT UUO group was significantly decreased in the *Sult1a1*-KO UUO group and further decreased in the *Sult1a1*-KO UUO+EPO group treated with rhEPO (Figure 8B). Sirius red staining revealed the same results as those observed for α-SMA expression (Figure 8C), indicating that the combination of *Sult1a1*-KO and rhEPO treatment might prevent renal fibrosis more effectively.

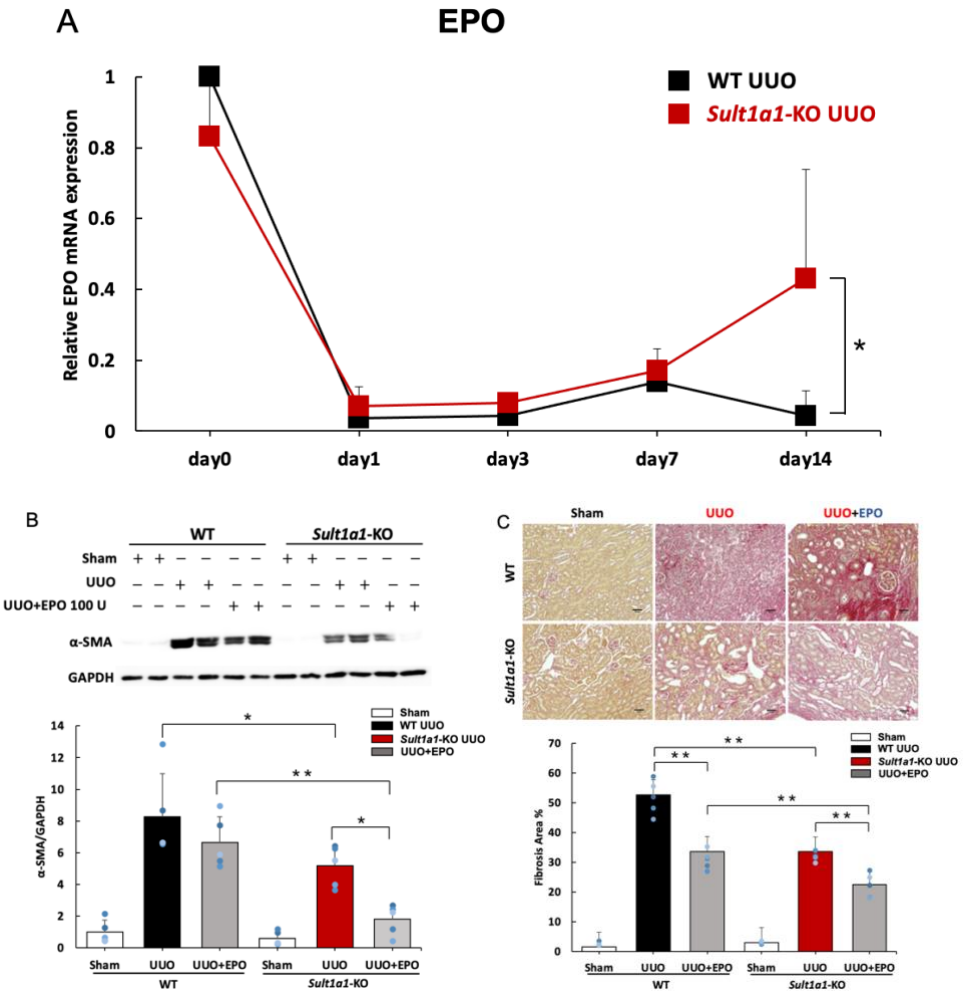

Figure 8. Effect of rhEPO treatment and *Sult1a1*-KO on renal fibrosis. (A) Time-dependent expression of EPO gene expression tested by RT-PCR. (B) Protein expression of α-SMA checked by western blot. (C) Collagen deposition (the red part) in the kidney confirmed by Sirius red staining. The scale bar = 50 μm. Each value represents the mean ± S.D. of 3–8 mice. *$p < 0.05$, **$p < 0.01$.

Chapter 4 Discussion

In this study, I investigated the pathological role of IS on renal fibrosis using *Sult1a1*-KO mice and the underlying mechanisms. *Sult1a1*-KO UUO mice exhibited reduced renal fibrosis, inflammation, and apoptosis and improved EPO production. $CD206^+$ macrophage infiltration prevents the progression of inflammation and renal fibrosis. The inactivation of Wnt/β-catenin signaling is involved in the decreased renal fibrosis process; treating *Sult1a1*-KO mice with rhEPO further attenuated UUO-induced renal fibrosis, indicating the possibility of combination therapy in patients with CKD.

IS accumulation has been linked to CKD progression. According to ultra-performance liquid chromatography-tandem mass spectrometry (UPLC-MS/MS) analysis, serum IS in healthy participants was ≤ 0.05–3.02 mg/L, and the average IS level progressively increased from 1.03 in CKD stage 1 to 12.21 mg/L in CKD stage 5.[37] However, there was no significant increase in serum BUN in the WT-UUO group (Figure 1A); *Sult1a1* mRNA expression and serum IS concentration were elevated in the WT UUO group (Figure 1B, C). It has been reported that the administration of IS (100 mg/kg/day, intraperitoneal) to healthy mice for three days significantly increased serum and kidney IS concentrations within three hours of the last administration.[38] This result indicates that IS is briefly retained in the serum and kidneys, even in normal renal function. In addition, human sulfotransferase SULT1A1 is a crucial phase II

xenobiotic-metabolizing enzyme that plays a vital role in sulfonating drugs, carcinogens, and steroids; it is highly expressed in the liver. The human sulfotransferase SULT1A1 is regulated by specificity protein 1 (Sp1) and GA-binding protein (GABP).[39] Elevated IS levels may affect Sp1- or GA-binding proteins and increase *Sult1a1* transcript levels in the liver. Therefore, the decreased elimination from UUO-treated kidneys may have caused a vicious cycle of increased *Sult1a1* transcription levels in the liver due to the accumulation of serum IS. Moreover, the administration of IS in animal CKD models increased IS retention in renal tubular cells and was accompanied by cell death in OAT1- and OAT3-expressing proximal tubular cells. [40] This effect could be rescued by probenecid, an anion transport inhibitor. Thus, inadequate renal clearance of IS during renal function decline may further aggravate IS-induced renal tubule cytotoxicity and accelerate CKD progression. Our results confirmed IS accumulation in the UUO mouse model; I hypothesized that the accumulated IS further affected renal fibrosis. Previous research established that combining benazepril (used to treat diabetic kidney disease) and AST-120 (which absorbs the precursor of IS in the intestine) reduces the progression of renal fibrosis in uremic rats,[41] which is consistent with our results in that a decrease in IS accumulation reduces renal fibrosis. In addition, IS activates mTORC1- and adenine-induced renal fibrosis, which was attenuated by AST-120 treatment.[38] All reports indicated that IS is related to renal fibrosis by several signal activation, consistent with

our results; however, different signaling pathways are involved due to the various stimuli to the kidneys.

IS was reported to involved in cardiovascular diseases through inducing oxidative stress and AST-120 treatment ameliorate the progression.[42-44] However, whether IS-induced oxidative stress is correlate with renal fibrosis has not been clearly discussed. Treated renal fibroblasts (NRK-49F) with IS (20 μM) induced the expression of collagen I and α-SMA, while fibroblast proliferation was not observed.[45] In human umbilical vein endothelial cells (HUVEC), IS inhibits NO production and cell viability by inducing ROS through induction of Nox4.[46] Nox4 presents a highest protein expression in normal human proximal tubular cells; its overexpression in mice tubular results in enhanced renal production of H_2O_2, however, this has no impact on renal fibrosis.[47] Therefore, other IS-related pathways not mediated by oxidative stress may be involved in reducing renal fibrosis in *Sult1a1*-KO mice.

According to animal model studies, the primary causes of renal fibrosis are uncontrolled epithelial damage and inflammation.[48] Based on these findings, I looked at the expression of inflammatory cytokines in WT and *Sult1a1*-KO mice kidneys. IL-6, TNF-α, and IL-1β levels increased in WT-UUO mice but decreased in *Sult1a1*-KO UUO mice, indicating that IS accumulation promotes inflammation in UUO kidneys; *Sult1a1*-KO UUO mice presented with infiltrated $CD206^+$ macrophages, which could play an anti-inflammatory role. When inflammation is ongoing, infiltrating leukocytes

activate intrinsic renal cells and cause the release of profibrotic cytokines and growth factors; consequently, myofibroblasts are recruited and activated, resulting in progressive renal fibrosis.[49] Therefore, I hypothesized that $CD206^{+}$ macrophages inhibit the ongoing inflammation and subsequent renal fibrosis *via* profibrotic cytokines and growth factor recruitment decrease.

On the other hand, genes associated with the Notch, Wnt, and Hedgehog signaling pathways are differentially expressed between patients with renal fibrosis and healthy control individuals, according to a genome-wide transcriptome investigation of kidneys from CKD and fibrosis patients.[50] In addition, after ischemia-reperfusion (IR) injury in mice, elevated Wnt ligand expression in isolated macrophages and an enhanced Wnt signaling response in epithelial cells were observed.[51] Wnt4 promotes tubular epithelial cell regeneration by regulating the cell-cycle proteins cyclin D1 and cyclin A.[52] Furthermore, lineage-tracing studies in mice revealed that Wnt4 expression was high in activated myofibroblasts, particularly in the medullary interstitium after UUO or IR injury.[50] In our study, the expression of Wnt4 was upregulated in UUO model, and *Sult1a1*-KO demonstrated no effect on Wnt4 expression, suggesting that Wnt4 is independent of IS-related renal fibrosis. Additionally, *Sult1a1*-KO mice exhibited elevated levels of sfrp5, which inhibits the Wnt signaling pathway by binding to Wnt protein. According to Yanlin Yu et al., IS increased renal fibrosis by downregulating sfrp5 expression and activating the Wnt/β-catenin signaling pathway;[53] this report

was consistent with the result of our study, confirming that sfrp5 was involved in IS-induced renal fibrosis. Therefore, the up-regulation of sfrp5 in *Sult1a1*-KO mice suppressed β-catenin activation, resulting in the prevention of fibrosis marker expression.

EPO is known to regulate the formation of red blood cells by stimulating bone marrow and is widely used for the clinical treatment of anemia.[54, 55] However, EPO unresponsiveness in several patients is common, suggesting that undefined causes affect anemia.[56] The accumulation of uremic toxins in blood impairs erythropoietin synthesis and compromising the growth and differentiation of red blood cells in the bone marrow.[57] IS has been reported to impair erythropoiesis by triggering apoptosis and senescence.[56] Our results revealed that EPO production was elevated in *Sult1a1*-KO mice (Figure 6A). Therapy targeting SULT1A1 may demonstrate the ability to treat the decreased EPO production capacity induced by UUO. Recent studies discovered that EPO might provide efficient protection against renal failure.[58] EPO significantly enhanced the recovery from acute renal failure induced by cisplatin in rats.[59] In rats with IR of the kidney, rhEPO was protective of the renal function and structure and the fibrosis and myofibroblast stimulation.[60] Consistently, our results indicate that *Sult1a1*-KO partly improved EPO production and progressive renal fibrosis was further suppressed by the administration of rhEPO to *Sult1a1*-KO mice. Although the treatment of EPO against renal fibrosis is under investigation, a high dose of EPO was found to

contribute to fibrogenesis in the long term.[60] Combining EPO treatment with IS suppression therapy might improve the issue.

Some concerns remain unanswered in our study, such as how IS activates inflammatory responses in the UUO model. Although the exact mechanism is unknown, IS is known to be a potent inducer of free radicals and may cause oxidative stress in the kidneys and cardiovascular system.[15, 61] Accordingly, I hypothesized that ureter obstruction causes IS accumulation, which can harm tubular cells by inducing oxidative stress, leading to the release of inflammatory cytokines. In addition, protein-bound uremic toxins contain 25 compounds.[62] Other than IS, PCS was produced mainly by *Sult1A1* in the liver, and its accumulation was related to decreased kidney function in CKD patients.[63] Its effect on renal fibrosis would be investigated using *Sult1a1*-KO mice in the future.

In conclusion, *Sult1a1*-KO mice demonstrated less IS build-up, which reduced UUO-induced renal fibrosis; infiltrating $CD206^{+}$ macrophages may aid inflammation and suppress renal fibrosis in *Sult1a1*-KO mice. Additionally, the inactivation of Wnt/β-catenin signaling helped slow the progression of renal fibrosis. Furthermore, in *Sult1a1*-KO mice, rhEPO administration suppressed renal fibrosis more effectively. Our findings confirmed the direct pathological role of IS in kidney inflammation and fibrosis, identifying SULT1A1 as a new therapeutic target for preventing or attenuating renal fibrosis (summarized in Figure 9).

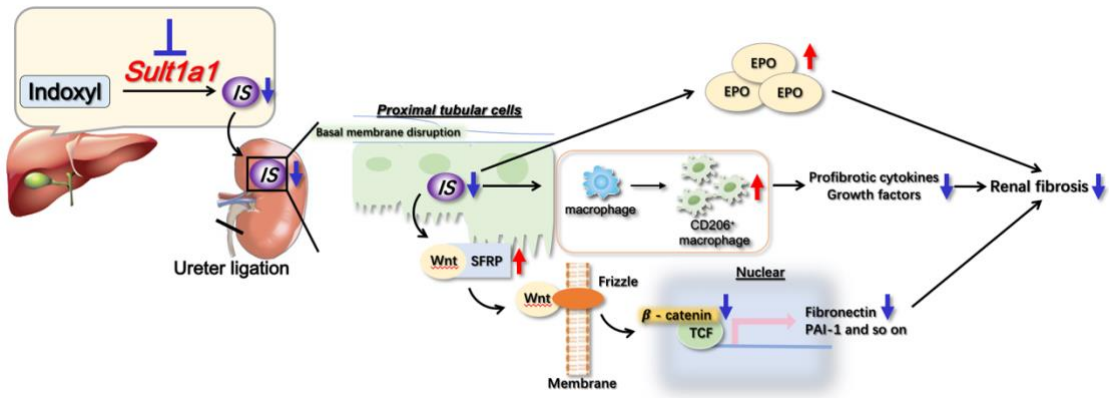

Figure 9. Summary of the mechanisms underlying UUO-induced renal fibrosis were suppressed in *Sult1a1*-KO mice. After unilater ureter was obstructed in *Sult1a1*-KO mice, IS accumulation was diminished in the serum and renal tissues due to lack of *Sult1a1* activity. UUO-induced renal fibrosis was suppressed accompanied by the decreased IS concentration. Furthermore, *Sult1a1* inhibition induced the infiltration of $CD206^{+}$ macrophages, which suppressed the ongoing inflammation and, as a result, renal firbrosis. Inactivated Wnt/β-catenin signaling and increased EPO production also help to reduce renal fibrosis.

Chapter 5 Materials and Methods

Sult1a1-KO mice

Sult1a1-deficient mouse embryos (Deltagen, America) were purchased, melted, and transplanted into an expedient parent at the Kumamoto University Institute of Resource Development and Analysis (IRDA) to manufacture the heteromouse. The mice were bred in the Animal Resources and Development (CARD) of Kumamoto University. Homogenized mice were then manufactured.

Animal experiments

All procedures for animal experiments were approved by the Kumamoto University ethical committee concerning animal experiments (Identification code: A 2019-046, Approval date: 2019) and were treated in accordance with the Guidelines of the United States National Institutes of Health regarding the care and use of animals for experimental procedures and the Guidelines of Kumamoto University for the care and use of laboratory animals. C57BL/6J mice at 7 weeks of age were housed in a standard animal maintenance facility at a constant temperature (22 ± 2 ℃) and humidity (50–70%) and a 12/12 - h light/dark cycle for approximately 1 week before the day of the experiment, with food and water available. The mice were anesthetized using isoflurane and placed on a heating plate (37 °C) to maintain a constant temperature. All surgeries

were conducted under isoflurane anesthesia, and all efforts were made to minimize animal suffering.

In protocol 1, C57BL/6J male mice (WT, 8-week-old) and *Sult1a1*-KO mice (8-week-old) were randomized and anesthetized before unilateral ureteral obstruction (UUO) treatment. WT and *Sult1a1*-KO mice were classified into four groups: WT Sham, WT UUO, *Sult1a1*-KO Sham, and *Sult1a1*-KO UUO groups. Each group contained 3–9 mice. The left ureter of each mouse was ligated with 3-0 silk, and the abdomen was closed with sutures. After surgery, the mice were warmed until recovery. The sham animals (control) underwent anesthesia and laparotomy only. The mice were sacrificed on day 14 after surgery (Figure 10).

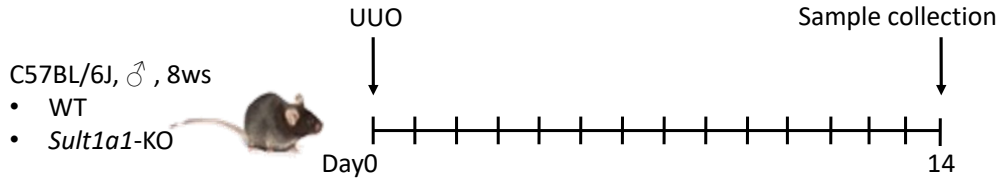

Figure 10. The protocol of a 2-week-UUO model

In protocol 2, group classification and UUO surgery were conducted as described in protocol 1. Each group contained 3–8 mice. To confirm the time-related changes in erythropoietin (EPO) levels in WT and *Sult1a1*-KO mice, mice were sacrificed on days 0, 1, 3, 7, and 14 following UUO surgery (Figure 11).

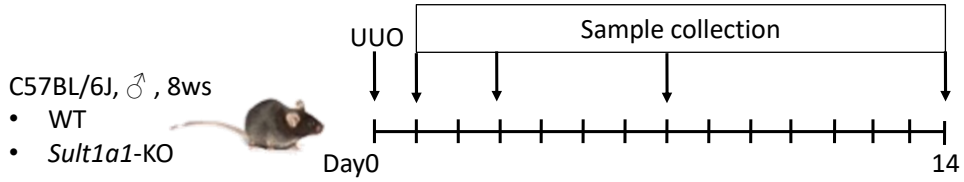

Figure 11. The protocol of collecting sample in a time-dependent way

In protocol 3, C57BL/6J male mice (WT, 8-week-olds) and *Sult1a1*-KO mice (8-week-olds) were randomized and anesthetized before UUO treatment. WT and *Sult1a1*-KO mice were classified into six groups: WT Sham, WT UUO, and WT UUO+EPO; *Sult1a1*-KO Sham, *Sult1a1*-KO UUO, and *Sult1a1*-KO UUO+EPO. Each group contained five mice. UUO surgery was performed as described in Protocol 1. Recombinant human erythropoietin (rhEPO) (R&D Systems) was diluted to 12.5 U/ml in sterile PBS (containing 0.1% bovine serum albumin) and administered intraperitoneally at 8 ml/kg every other day starting on day 3 after UUO treatment. Sterile PBS containing 0.1% bovine serum albumin was used as the control. The mice were sacrificed on day 14 after surgery (Figure 12).

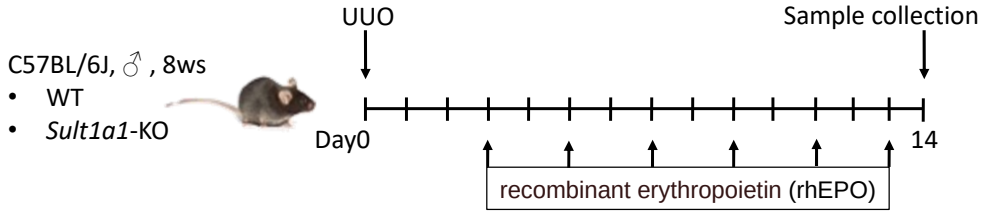

Figure 12. The protocol of treating 2-week-UUO mice with rhEPO.

Sample collection

Blood was collected on day 14 and centrifuged at 3,000 g for 10 min to obtain serum samples. Serum BUN concentration was measured using a Fuji Dry Chem Nx500 (Fujifilm, Kanagawa, Japan). The kidneys and liver were collected on day 14. One part of the kidney was fixed in neutral-buffered formalin and embedded in paraffin. The

remaining kidney was used for western blotting and RT-PCR analysis. All samples were stored at –80 °C until analysis.

Liquid chromatography/mass spectrometry/MS (LC-MS/MS) assay of IS concentration

Kidney tissue (30 mg) was homogenized in 200 μL PBS and centrifuged at 3,000 g for 10 min at 4 °C to obtain tissue samples. The Standard and samples (12.5 μL) were added to 87.5 μL acetonitrile. The samples were vortexed and centrifuged at 161,769 g for 10 min at 4 °C to remove the proteins. The supernatant (25 μL) was added to the liquid phase (10 μM ammonium acetate solution). The mixture was vortexed and centrifuged at 161,769 g for 10 minutes at 4 °C. Next, the supernatant (40 μL) was injected into the LC-MS/MS system. Aliquots of the extracts (5 μL) were separated on a SymmetryTM C18 (5 μm, 3.9×150 mm) column (Waters Corp, Milford, MA, USA) interfaced with an API3200TM LC-MS/MS system (AB SCIEX, Foster City, CA, USA) operating in negative TurboIonSpray mode. The samples were eluted at a flow rate of 0.2 mL/min using a mobile phase of 10 mM ammonium acetate: acetonitrile (73:27 v/v) at 40 °C.

Sirius red staining

Sirius red staining was performed for collagen deposition analysis. The tissue of mouse kidneys harvested on day 14 after obstruction was fixed in 10% phosphate-buffered formaldehyde for 48 h, embedded in paraffin, sectioned (4 μm), deparaffinized with xylene, rehydrated through a graded series of ethanol, and then washed in water. Adequate picrosirius red solution was applied to cover the tissue section completely and incubated for 60 min. The slides quickly with two changes of 0.5% Acetic Acid Solution. The slides were then rinsed using absolute alcohol, dehydrated in two changes of absolute alcohol, cleared, and mounted in synthetic resin. The percentage of collagen deposition area versus the whole tissue area was calculated using the all-in-one fluorescence microscope BZ-X700 (×200 magnification) (KEYENCE). Five areas in each section were calculated for each mouse. Data from the mice in the same treatment groups were averaged.

TUNEL staining

Kidney specimens from WT and *Sult1a1*-KO mice were stained using an *in situ* apoptosis detection kit (Takara Bio Inc., Shiga, Japan). Under light microscopy (×200 magnification), the number of TUNEL-positive cells in the area covering the majority of corticomedullary junctions in a slide was counted by researchers blinded to the

samples. The number of TUNEL-positive cells in five sections from each mouse was counted. Data from the mice in the same treatment groups were averaged.

Dihydroethidium (DHE) staining

Dihydroethidium (DHE) (Fujifilm) is oxidized by intracellular ROS to form ethidium, which in turn intercalates with DNA inside the nucleus, giving nuclear staining to ROS-positive cells. OCT-embedded kidney tissues were sectioned (10 μm), dried in silica gel (Wako). Incubation with DHE at 30 min in a room temperature. Slides were rinsed in PBS and then observed under all-in-one fluorescence microscope BZ-X700 (×200 magnification) (KEYENCE).

Immunostaining

Kidney specimens from WT and *Sult1a1*-KO mice were deparaffinized with xylene, rehydrated using a graded series of ethanol, and then washed in water. To quench endogenous peroxidase activity, tissues were incubated tissues with 3% H_2O_2 in PBS for 10 min. The slides were then rinsed in PBS for 3 min. The primary antibody 4-HNE (ab46545, abcam), 8-OHdG (sc-66036, Santa Cruz), $CD206^+$ (MR5D3, Thermo Fisher Scientific) was applied at 4 °C overnight. The slides were then rinsed in PBS three times for 5 min. The secondary antibody was applied at room temperature for 1 h. The slides were then rinsed in PBS three times for 5 min. The required working volume of

DAB/AEC Chromogen Solution was provided since 100–200 μL was required to cover the entire tissue section on a single slide. About 1–5 drops of DAB Chromogen Solution were added to cover the entire tissue section and then incubated for 5 min. The slides were rinsed, dehydrated, and mounted. The intensity of the tissue staining was monitored under a light microscope. The $CD206^+$ area was calculated using an all-in-one fluorescence microscope BZ-X700 (×200 magnification) (KEYENCE). Five areas in each section were calculated for each mouse. Data from the mice in the same treatment groups were averaged.

Western blot analysis

Kidneys were homogenized in 1x RIPA buffer. Protein content was measured using a bicinchoninic acid (BCA) protein assay reagent (Thermo Fisher Scientific, Waltham, MA, USA). Each sample was mixed in loading buffer (2 w/v % sodium dodecyl sulfate (SDS), 125 mM Tris-HCl pH 7.2, 20 v/v % glycerol, and 5 v/v % 2- mercaptoethanol) and heated at 95 °C for 2 min. The samples were subjected to sodium dodecyl sulfate-polyacrylamide gel electrophoresis using a 10% gel and transferred onto a polyvinylidene difluoride membrane (Immobilon-P; EMD Millipore, Billerica, MA, USA) by semidry electro-blotting. The membrane was blocked for 1 h at room temperature with 2 v/v % ECL Advance Blocking Agent (GE Healthcare UK Ltd., Little Chalfont, UK) in 50 mM Tris-buffered saline (pH 7.6) containing 0.3 v/v % Tween 20,

and then incubated for 1 h at room temperature with a primary antibody specific for α-SMA (ab5694, abcam), b-catenin (ab32572, abcam) or GAPDH (ab199713, abcam). The blots were washed with Tris-buffered saline containing Tween 20 before incubation with the secondary antibody (horseradish peroxidase-labeled anti-rabbit immunoglobulin F(ab)2 or horseradish peroxidase-linked anti-mouse immunoglobulin F(ab)2) (GE Healthcare Ltd., Chicago, IL, USA) for 1 h at room temperature. Immunoblots were visualized using an ECL system (ECL Advance Western Blotting Detection Kit; GE Healthcare Ltd., Chicago, IL, USA). The dilutions of the antibodies are presented in Table 1. The dilution agent used was 5% v/v Nonfat Dry Milk.

Table 1. Dilution of antibody

Target protein	The primary antibody	The secondary antibody
α-SMA	Dilution: 5,000 x	Dilution: 20,000 x
β-catenin	Dilution: 5,000 x	Dilution: 10,000 x
GAPDH	Dilution: 5,000 x	Dilution: 5,000 x

Real-time PCR

Total RNA was isolated from the kidneys using TRIzol (Invitrogen. Tokyo, Japan) according to the manufacturer’s protocol. cDNA synthesis was performed using the PrimeScript RT Reagent Kit Perfect Real Time (TAKARA BIO INC.Shiga, Japan). Real-time PCR analysis of Col1a1, TGF-β1, PAI-1, fibronectin, IL-6, Wnt4, sfrp5 and GAPDH was performed in a LightCycler® 480 System II using SYBR® Premix DimerEraser® Perfect Real Time (TaKaRa Bio Inc.). The PCR amplifications were performed under the following conditions: initialization for 30 s at 95 °C, followed by 50 cycles of amplification, with 5 s at 95 °C for denaturation, and 30 s at 72 °C for annealing and elongation. The primers (NIHON GENE RESEARCH LABORATORIES Inc.) used for the mice are presented in Table 2. The threshold cycle (Ct) values for each gene amplification were normalized by subtracting the Ct value for GAPDH. The normalized gene expression values are expressed as the relative quantity of gene-specific mRNA compared to GAPDH.

Table 2. Primer sequences for each gene

Gene	Forward (5'-3')	Reverse (5'-3')
Sult1a1	TGAGACGCACTCACCCTGTTCT	TCCACAGTCTCCTCAGGTAGAG
Col1a1	GACAAATGAATGGGGCAAG	CAATGTCCAGAGGTGCAATG
IL-6	TACCACTTCACAAGTCGGAGGC	CTGCAAGTGCATCATCGTTGTTC
TNF-α	CTACCTTGTTGCCTCCTCTTT	GAGCAGAGGTTCAGTGATGTAG
IL-1β	AGTTGACGGACCCCAAAAG	AGCTGGATGCTCTCATCAGG
AhR	AGGCTAAGAGAGCCTTGTCT	TCCAACACTTTCTGGACAGG
HO-1	AACAAGCAGAACCCAGTCTATGC	AGGTAGCGGGTATATGCGTGGGCC
XO	GCTCTTCGTGAGCACACAGAAC	CCACCCATTCTTTTCACTCGGAC
Nox1	CTCCAGCCTATCTCATCCTGAG	AGTGGCAATCACTCCAGTAAGGC
Nox2	TGGCGATCTCAGCAAAAGGTGG	GTACTGTCCCACCTCCATCTTG
F4/80	CGTGTTGTTGGTGGCACTGTGA	CCACATCAGTGTTCCAGGAGAC
$CD206^{+}$	GTTCACCTGGAGTGATGGTTCTC	AGGACATGCCAGGGTCACCTTT
Wnt4	GCGTAGCCTTCTCACAGTCC	CGCATGTGTGTCAAGATGG
sFRP5	GATCTGTGCCCAGTGTGAGA	TATGCAGGACCAGCTTCTTGGTGT
β-catenin	GCAGCAGCAGTCTTACTTGG	CCCTCATCTAGCGTCTCAGG
Fibronectin	AGACCATACCTGCCGAATGTAG	GAGAGCTTCCTGTCCTGTAGAG
EPO	CACAACCCATCGTGACATTTTC	CATCTGCGACAGTCGAGTTCTG
GAPDH	CGACTTCAACAGCAACTCCCACTC TTCC	TGGGTGGTCCAGGGTTTCTTACTC CTT

Statistical analysis

Data were statistically analyzed by analysis of variance, followed by Tukey's or Scheffé's multiple comparisons test, using Statcel2 software (OMS Ltd., Saitama, Japan). Statistical p-value <0.05 was considered statistically significant. All data are presented as mean $\pm$ standard deviation (SD).

Reference

1. Zhang L, Zhang P, Wang F*, et al.* Prevalence and factors associated with CKD: a population study from Beijing. Am J Kidney Dis 2008;51(3):373-384
2. Sharma SK, Zou H, Togtokh A*, et al.* Burden of CKD, proteinuria, and cardiovascular risk among Chinese, Mongolian, and Nepalese participants in the International Society of Nephrology screening programs. Am J Kidney Dis 2010;56(5):915-927
3. Kovesdy CP. Epidemiology of chronic kidney disease: an update 2022. Kidney Int Suppl (2011) 2022;12(1):7-11
4. Lv JC, Zhang LX. Prevalence and Disease Burden of Chronic Kidney Disease. Adv Exp Med Biol 2019;1165:3-15
5. Zhao X, Kwan JYY, Yip K*, et al.* Targeting metabolic dysregulation for fibrosis therapy. Nat Rev Drug Discov 2020;19(1):57-75
6. Liu Y. Cellular and molecular mechanisms of renal fibrosis. Nat Rev Nephrol 2011;7(12):684-696
7. Miyazaki T, Ise M, Hirata M*, et al.* Indoxyl sulfate stimulates renal synthesis of transforming growth factor-beta 1 and progression of renal failure. Kidney Int Suppl 1997;63:S211-214
8. Niwa T, Ise M. Indoxyl sulfate, a circulating uremic toxin, stimulates the progression of glomerular sclerosis. J Lab Clin Med 1994;124(1):96-104
9. Shimoishi K, Anraku M, Kitamura K*, et al.* An oral adsorbent, AST-120 protects against the progression of oxidative stress by reducing the accumulation of indoxyl sulfate in the systemic circulation in renal failure. Pharm Res 2007;24(7):1283-1289
10. Saito H, Yoshimura M, Saigo C*, et al.* Hepatic sulfotransferase as a nephropreventing target by suppression of the uremic toxin indoxyl sulfate accumulation in ischemic acute kidney injury. Toxicol Sci 2014;141(1):206-217
11. Saigo C, Nomura Y, Yamamoto Y*, et al.* Meclofenamate elicits a nephropreventing effect in a rat model of ischemic acute kidney injury by suppressing indoxyl sulfate production and restoring renal organic anion transporters. Drug Des Devel Ther 2014;8:1073-1082
12. Lin CJ, Chen HH, Pan CF*, et al.* p-Cresylsulfate and indoxyl sulfate level at different stages of chronic kidney disease. J Clin Lab Anal 2011;25(3):191-197
13. Takkavatakarn K, Phannajit J, Udomkarnjananun S*, et al.* Association Between Indoxyl Sulfate and Dialysis Initiation and Cardiac Outcomes in Chronic Kidney Disease Patients. Int J Nephrol Renovasc Dis 2022;15:115-126
14. Niwa T. Removal of protein-bound uraemic toxins by haemodialysis. Blood Purif 2013;35 Suppl 2:20-25
15. Niwa T. Role of indoxyl sulfate in the progression of chronic kidney disease and

cardiovascular disease: experimental and clinical effects of oral sorbent AST-120. Ther Apher Dial 2011;15(2):120-124
16. Gelasco AK, Raymond JR. Indoxyl sulfate induces complex redox alterations in mesangial cells. Am J Physiol Renal Physiol 2006;290(6):F1551-1558
17. Fukuda Y, Takazoe M, Sugita A, *et al.* Oral spherical adsorptive carbon for the treatment of intractable anal fistulas in Crohn's disease: a multicenter, randomized, double-blind, placebo-controlled trial. Am J Gastroenterol 2008;103(7):1721-1729
18. Yabuuchi N, Hou H, Gunda N, *et al.* Suppressed Hepatic Production of Indoxyl Sulfate Attenuates Cisplatin-Induced Acute Kidney Injury in Sulfotransferase 1a1-Deficient Mice. Int J Mol Sci 2021;22(4)
19. Iwata K, Watanabe H, Morisaki T, *et al.* Involvement of indoxyl sulfate in renal and central nervous system toxicities during cisplatin-induced acute renal failure. Pharm Res 2007;24(4):662-671
20. Morisaki T, Matsuzaki T, Yokoo K, *et al.* Regulation of renal organic ion transporters in cisplatin-induced acute kidney injury and uremia in rats. Pharm Res 2008;25(11):2526-2533
21. Li X, Pan J, Li H, *et al.* DsbA-L mediated renal tubulointerstitial fibrosis in UUO mice. Nat Commun 2020;11(1):4467
22. Liao X, Lv X, Zhang Y, *et al.* Fluorofenidone Inhibits UUO/IRI-Induced Renal Fibrosis by Reducing Mitochondrial Damage. Oxid Med Cell Longev 2022;2022:2453617
23. Aranda-Rivera AK, Cruz-Gregorio A, Aparicio-Trejo OE, *et al.* Redox signaling pathways in unilateral ureteral obstruction (UUO)-induced renal fibrosis. Free Radic Biol Med 2021;172:65-81
24. Vaughan ED, Jr., Marion D, Poppas DP, *et al.* Pathophysiology of unilateral ureteral obstruction: studies from Charlottesville to New York. J Urol 2004;172(6 Pt 2):2563-2569
25. Docherty NG, O'Sullivan OE, Healy DA, *et al.* Evidence that inhibition of tubular cell apoptosis protects against renal damage and development of fibrosis following ureteric obstruction. Am J Physiol Renal Physiol 2006;290(1):F4-13
26. Lv W, Booz GW, Wang Y, *et al.* Inflammation and renal fibrosis: Recent developments on key signaling molecules as potential therapeutic targets. Eur J Pharmacol 2018;820:65-76
27. Ikezumi Y, Suzuki T, Hayafuji S, *et al.* The sialoadhesin (CD169) expressing a macrophage subset in human proliferative glomerulonephritis. Nephrol Dial Transplant 2005;20(12):2704-2713
28. Eardley KS, Kubal C, Zehnder D, *et al.* The role of capillary density, macrophage infiltration and interstitial scarring in the pathogenesis of human chronic kidney disease. Kidney Int 2008;74(4):495-504
29. Anders HJ, Ryu M. Renal microenvironments and macrophage phenotypes

determine progression or resolution of renal inflammation and fibrosis. Kidney Int 2011;80(9):915-925
30. Nakano T, Katsuki S, Chen M*, et al.* Uremic Toxin Indoxyl Sulfate Promotes Proinflammatory Macrophage Activation Via the Interplay of OATP2B1 and Dll4-Notch Signaling. Circulation 2019;139(1):78-96
31. He W, Dai C, Li Y*, et al.* Wnt/beta-catenin signaling promotes renal interstitial fibrosis. J Am Soc Nephrol 2009;20(4):765-776
32. Arinze NV, Yin W, Lotfollahzadeh S*, et al.* Tryptophan metabolites suppress the Wnt pathway and promote adverse limb events in chronic kidney disease. J Clin Invest 2022;132(1)
33. Luo C, Zhou S, Zhou Z*, et al.* Wnt9a Promotes Renal Fibrosis by Accelerating Cellular Senescence in Tubular Epithelial Cells. J Am Soc Nephrol 2018;29(4):1238-1256
34. Asada N, Takase M, Nakamura J*, et al.* Dysfunction of fibroblasts of extrarenal origin underlies renal fibrosis and renal anemia in mice. J Clin Invest 2011;121(10):3981-3990
35. Souma T, Yamazaki S, Moriguchi T*, et al.* Plasticity of renal erythropoietin-producing cells governs fibrosis. J Am Soc Nephrol 2013;24(10):1599-1616
36. Chiang CK, Tanaka T, Inagi R*, et al.* Indoxyl sulfate, a representative uremic toxin, suppresses erythropoietin production in a HIF-dependent manner. Lab Invest 2011;91(11):1564-1571
37. Farris AB, Colvin RB. Renal interstitial fibrosis: mechanisms and evaluation. Curr Opin Nephrol Hypertens 2012;21(3):289-300
38. Nakano T, Watanabe H, Imafuku T*, et al.* Indoxyl Sulfate Contributes to mTORC1-Induced Renal Fibrosis via The OAT/NADPH Oxidase/ROS Pathway. Toxins (Basel) 2021;13(12)
39. Hempel N, Wang H, LeCluyse EL*, et al.* The human sulfotransferase SULT1A1 gene is regulated in a synergistic manner by Sp1 and GA binding protein. Mol Pharmacol 2004;66(6):1690-1701
40. Granados JC, Bhatnagar V, Nigam SK. Blockade of Organic Anion Transport in Humans After Treatment With the Drug Probenecid Leads to Major Metabolic Alterations in Plasma and Urine. Clin Pharmacol Ther 2022;112(3):653-664
41. Aoyama I, Shimokata K, Niwa T. Combination therapy with benazepril and oral adsorbent ameliorates progressive renal fibrosis in uremic rats. Nephron 2002;90(3):297-312
42. Yisireyili M, Shimizu H, Saito S*, et al.* Indoxyl sulfate promotes cardiac fibrosis with enhanced oxidative stress in hypertensive rats. Life Sci 2013;92(24-26):1180-1185
43. Yu M, Kim YJ, Kang DH. Indoxyl sulfate-induced endothelial dysfunction in patients with chronic kidney disease via an induction of oxidative stress. Clin J Am

Soc Nephrol 2011;6(1):30-39
44. Niwa T. Indoxyl sulfate is a nephro-vascular toxin. J Ren Nutr 2010;20(5 Suppl):S2-6
45. Milanesi S, Garibaldi S, Saio M*, et al.* Indoxyl Sulfate Induces Renal Fibroblast Activation through a Targetable Heat Shock Protein 90-Dependent Pathway. Oxid Med Cell Longev 2019;2019:2050183
46. Tumur Z, Niwa T. Indoxyl sulfate inhibits nitric oxide production and cell viability by inducing oxidative stress in vascular endothelial cells. Am J Nephrol 2009;29(6):551-557
47. Rajaram RD, Dissard R, Faivre A*, et al.* Tubular NOX4 expression decreases in chronic kidney disease but does not modify fibrosis evolution. Redox Biol 2019;26:101234
48. Tecklenborg J, Clayton D, Siebert S*, et al.* The role of the immune system in kidney disease. Clin Exp Immunol 2018;192(2):142-150
49. Wang YY, Jiang H, Pan J*, et al.* Macrophage-to-Myofibroblast Transition Contributes to Interstitial Fibrosis in Chronic Renal Allograft Injury. J Am Soc Nephrol 2017;28(7):2053-2067
50. Edeling M, Ragi G, Huang S*, et al.* Developmental signalling pathways in renal fibrosis: the roles of Notch, Wnt and Hedgehog. Nat Rev Nephrol 2016;12(7):426-439
51. Kawakami T, Ren S, Duffield JS. Wnt signalling in kidney diseases: dual roles in renal injury and repair. J Pathol 2013;229(2):221-231
52. Terada Y, Tanaka H, Okado T*, et al.* Expression and function of the developmental gene Wnt-4 during experimental acute renal failure in rats. J Am Soc Nephrol 2003;14(5):1223-1233
53. Yu Y, Guan X, Nie L*, et al.* DNA hypermethylation of sFRP5 contributes to indoxyl sulfate-induced renal fibrosis. J Mol Med (Berl) 2017;95(6):601-613
54. Bhoopalan SV, Huang LJ, Weiss MJ. Erythropoietin regulation of red blood cell production: from bench to bedside and back. F1000Res 2020;9
55. Moore E, Bellomo R. Erythropoietin (EPO) in acute kidney injury. Ann Intensive Care 2011;1(1):3
56. Duangchan T, Rattanasompattikul M, Chitchongyingcharoen N*, et al.* Indoxyl sulfate impairs in vitro erythropoiesis by triggering apoptosis and senescence. Exp Biol Med (Maywood) 2022;247(15):1350-1363
57. Hamza E, Metzinger L, Metzinger-Le Meuth V. Uremic Toxins Affect Erythropoiesis during the Course of Chronic Kidney Disease: A Review. Cells 2020;9(9)
58. Spandou E, Tsouchnikas I, Karkavelas G*, et al.* Erythropoietin attenuates renal injury in experimental acute renal failure ischaemic/reperfusion model. Nephrol Dial Transplant 2006;21(2):330-336

59. Dodds A, Nicholls M. Haematological aspects of renal disease. Anaesth Intensive Care 1983;11(4):361-368
60. Gobe GC, Bennett NC, West M*, et al.* Increased progression to kidney fibrosis after erythropoietin is used as a treatment for acute kidney injury. Am J Physiol Renal Physiol 2014;306(6):F681-692
61. Fujii H, Nakai K, Fukagawa M. Role of oxidative stress and indoxyl sulfate in progression of cardiovascular disease in chronic kidney disease. Ther Apher Dial 2011;15(2):125-128
62. Vanholder R, De Smet R, Glorieux G*, et al.* Review on uremic toxins: classification, concentration, and interindividual variability. Kidney Int 2003;63(5):1934-1943
63. Rong Y, Kiang TKL. Characterization of human sulfotransferases catalyzing the formation of p-cresol sulfate and identification of mefenamic acid as a potent metabolism inhibitor and potential therapeutic agent for detoxification. Toxicol Appl Pharmacol 2021;425:115553

Acknowledgement

I would like to express my deepest gratitude to Professor Hideyuki Saito of the Department of Pharmacy, Kumamoto University Hospital, for his wisdom guidance and encouragement throughout this research.

I would like to express my heartfelt appreciation to Associate Professor Hirofumi Jono of the Department of Pharmacy, Kumamoto University Hospital, for his counsel and support throughout this research.

I would like to express my sincere gratitude to Assistant Professor Yuki Narita of the Department of Pharmacy, Kumamoto University Hospital, for his kind advice and assistance throughout this research.

As an overseas student, I would like to thank the students of the Department of Clinical Pharmacokinetics, Faculty of Pharmaceutical Sciences, Kumamoto University, for their understanding and cooperation throughout this research.

Finally, I would like to thank my family and friends who have supported me and warmly watched over me.